# SUPPLEMENTARY INFORMATION

## Enzyme Assembly on Nanoparticle Scaffolds Enhances Cofactor Recycling and Improves Coupled Reaction Kinetics

Joyce C. Breger[1], Ellen R. Goldman[1], Kimihiro Susumu[2], Eunkeu Oh[2],

Christopher M. Green[1], Shelby L. Hooe[1,3], Meghna Thakur[1,4],

Igor L. Medintz[1], and Gregory A. Ellis[1]*

[1]Center for Bio/Molecular Science and Engineering Code 6900
[2]Optical Sciences Division Code 5600
U.S. Naval Research Laboratory
Washington, D.C., 20375, USA

[3]National Research Council
Washington, D.C., 20001, USA

[4]College of Science
George Mason University
Fairfax, Virginia, 22030 USA

*Email: Gregory.ellis@nrl.navy.mil

**Keywords:** Enzyme, catalysis, nanoparticle, quantum dot, substrate channeling, glucose dehydrogenase, cofactor recycling, NADH.

**Supplementary Table S1. Estimated GDH Kinetic Parameters Measured On and Off QDs for $NADP^+$ as cofactor with glucose as substrate.**

| Ratio GDH per QD | $V_{Max}$ | $k_{cat}$ | $K_M$ | $k_{cat}/K_M$ |
|---|---|---|---|---|
| **Substrate: Glucose**[a,b,c] | **(nM × $s^{-1}$)** | **($s^{-1}$)** | **(μM)** | **($mM^{-1}$ × $s^{-1}$)** |
| 0 | 22.3 ± 3.7 | 4.70 ± 0.77 | 8535 ± 3580 | 0.55 ± 0.25 |
| 1 | 82.8 ± 7.3 | 17.43 ± 1.53 | 4919 ± 1308 | 3.54 ± 0.99 |
| 2 | 82.7 ± 5.6 | 17.40 ± 1.18 | 5723 ± 1127 | 3.04 ± 0.63 |
| 4 | 72.3 ± 4.4 | 15.22 ± 0.92 | 6340 ± 1087 | 2.40 ± 0.44 |
| 8 | 77.1 ± 2.2 | 16.24 ± 0.46 | 6632 ± 526 | 2.45 ± 0.21 |
| 16 | 63.8 ± 5.8 | 13.44 ± 1.21 | 8009 ± 1910 | 1.68 ± 0.43 |
| 32 | 30.6 ± 0.8 | 6.44 ± 0.17 | 9771 ± 623 | 0.66 ± 0.05 |

Final enzyme concentrations: [a]GDH = 5 nM, [b]glucose = 35 mM, starting [b]$NADP^+$ = 700 μM. Buffer = 100 mM phosphate pH 8. All kinetic values are qualified as apparent.[1, 2]

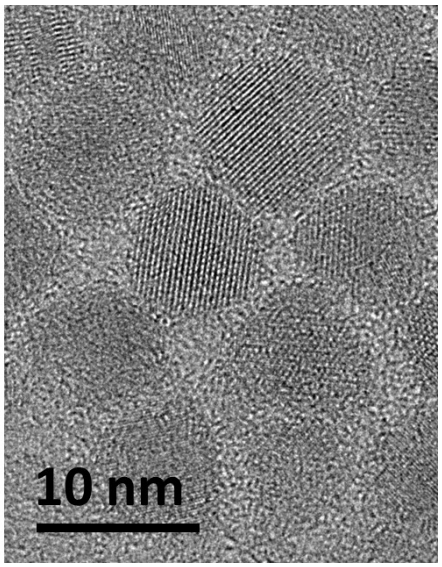


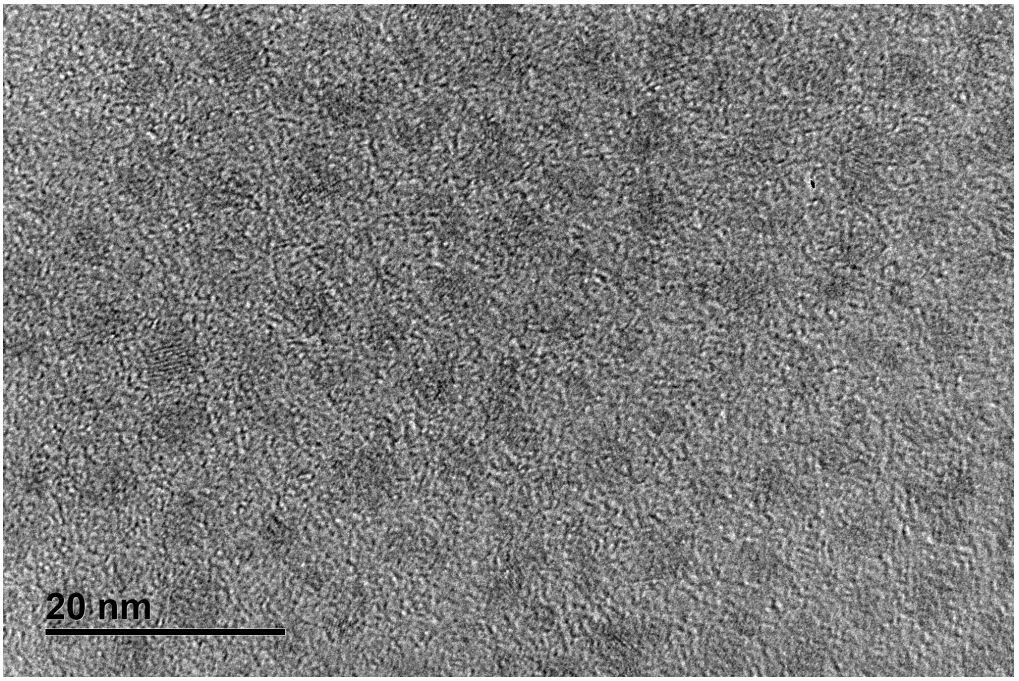


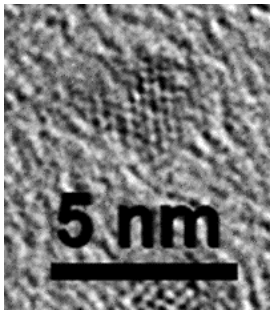


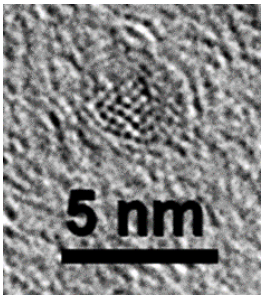


**Supplementary Figure S1. (Top)** Representative high-resolution TEM micrograph of 625 QDs. **(Bottom)** Representative high-resolution TEM micrograph of 523 QDs showing their lack of aggregation when enzymes are not present.

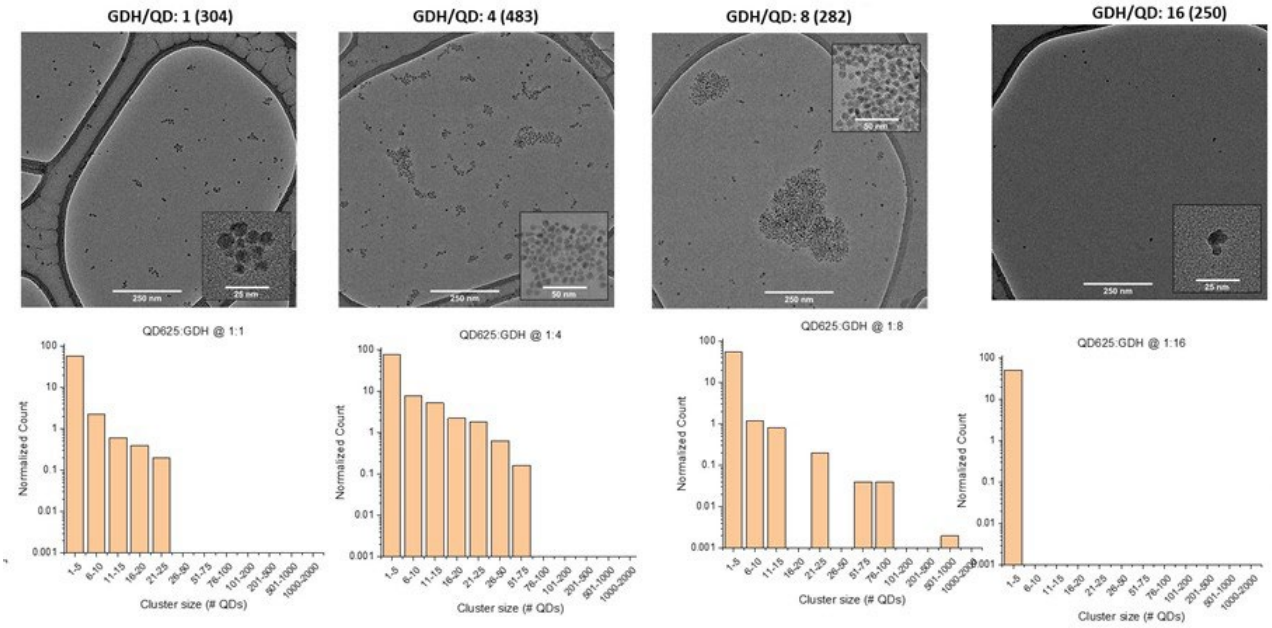


**Supplementary Figure S2.** Representative TEM micrographs of 625 nm emitting QDs (~9.7 nm diameter) assembled with a ratio of 1, 4, 8, and 16 GDH proteins per QD. Inset in each shows a high resolution image of a cluster. Also provided with the ratios above each micrograph is the number of QDs or aggregates counted for cluster size analysis. Analysis of QD cluster sizes (number of QDs present in the cluster) observed plotted below each micrograph using the indicated bin sizes for cluster groups.

**PAGE analysis:**

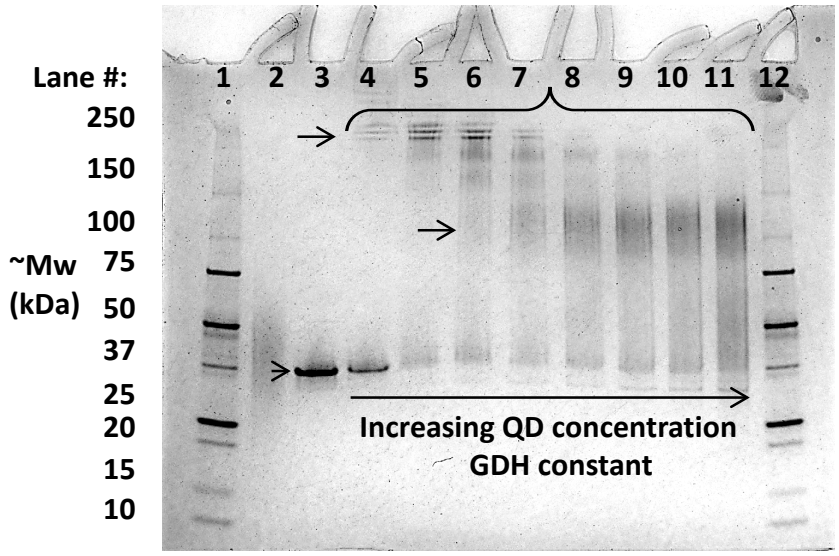


**Gel Contents:**
Lane 1 and Lane 12: Protein marker
Lane 2: QD 100 pmol
Lane 3: GDH 20 pmol (28 kDa monomer)
Lane 4: GDH 20 pmol + QD 0.8 pmol
Lane 5: GDH 20 pmol + QD 1.6 pmol
Lane 6: GDH 20 pmol + QD 3.2 pmol
Lane 7: GDH 20 pmol + QD 6.3 pmol
Lane 8: GDH 20 pmol + QD 12.5 pmol
Lane 9: GDH 20 pmol + QD 25 pmol
Lane 10: GDH 20 pmol + QD 50 pmol
Lane 11: GDH 20 pmol + QD 100 pmol

**Supplementary Figure S3.** 4-12% gradient PAGE gel showing separation of GDH as free in solution and then as complexed to the indicated increasing ratio of QD. GDH migrates as the ~28 kDa monomer rather than as the tetramer, see bottom arrow lane 3. The QDs do not appear under commassie blue staining used here. Upon addition of QD, a higher molecule weight (MW) band of ~250 kDa appears for lanes 4-7 at the interface between the upper loading gel and bottom separation gel indicating cross-linked protein aggregates that did not migrate into the separating portion of the gel. Another smear of high MW species appear in lanes 6-11 between 75 and 150 kDa, which also gets darker with increasing QD presence. The protein monomer species also disappears even with only 1.6 pmol of QD added. These high MW species represent the different distributions of QD-GDH nanoaggregates or clusters. Similar to that shown in previous reports, protein depletion as a function of increasing QD concentration is used here as evidence of cluster formation.[3] It is also probable that enzymes that are somewhat 'loosely' associated with the clusters may get partially stripped from the nanocluster as they separate in the gel.

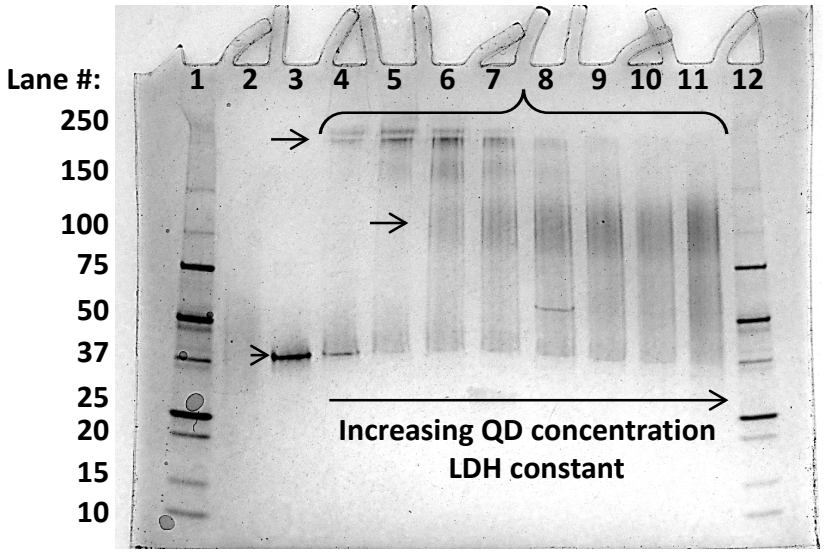


**Gel Contents:**

Lane 1 and Lane 12: Protein marker
Lane 2: QD 100 pmol
Lane 3: LDH 20 pmol (38.7 kDa monomer)
Lane 4: LDH 20 pmol + QD 0.8 pmol
Lane 5: LDH 20 pmol + QD 1.6 pmol
Lane 6: LDH 20 pmol + QD 3.2 pmol
Lane 7: LDH 20 pmol + QD 6.3 pmol
Lane 8: LDH 20 pmol + QD 12.5 pmol
Lane 9: LDH 20 pmol + QD 25 pmol
Lane 10: LDH 20 pmol + QD 50 pmol
Lane 11: LDH 20 pmol + QD 100 pmol

**Supplementary Figure S4.** 4-12% gradient PAGE gel showing separation of LDH as free in solution and then as complexed to the indicated increasing ratio of QD. LDH migrates as the 38.7 kDa monomer rather than as the tetramer, see bottom arrow lane 3. The QDs do not appear under commassie blue staining used here. Upon addition of QD, a higher molecule weight (MW) band of ~250 kDa appears for lanes 4-7 at the interface between the upper loading gel and bottom separation gel indicating protein aggregates that did not migrate into the separating portion of the gel. Another smear of high MW species appear in lanes 6-11 between 75 and 150 kDa, which also gets darker with increasing QD presence. The protein monomer species also disappears even with only 1.6 pmol of QD added. These high MW species represent the different distributions of QD-LDH nanoaggregates or clusters. Protein depletion as a function of increasing QD concentration is used here as evidence of cluster formation. It is also probable that enzymes that are somewhat 'loosely' associated with the clusters may get partially stripped from the nanocluster as they separate in the gel.

*Glucose Dehydrogenase Stability Assay.* Previous data had indicated that some multimeric enzymes such as LDH in particular can fall apart and monomerize at low concentration thus losing activity. In contrast to this, LDH remained active when assembled to and cross-linked by QDs even at concentrations far below that where the free enzyme lost activity.[3] This assay was meant to test the stability of GDH tertiary structure in solution and when attached to QDs in a similar manner. For this assay, decreasing amounts of GDH were assembled to 523 QD's to maintain a ratio of either 0.5 or 1 GDH per QD. The final QD concentration ranged from 1 to 200 nM with GDH concentrations either the same or 0.5× that of the QD. Constructs were allowed to assemble in 100 mM phosphate buffer for at least 1 hr prior to being aliquoted into a 384-well microtiterwell plate. Substrate solution consisted of a final concentration of 840.9 μM $NAD^+$ and 33.7 μM glucose. The reaction was monitored in a plate reader as described in the manuscript with each condition performed in quadruplicate. Initial rates were determined from the linear portions of the reaction curves.

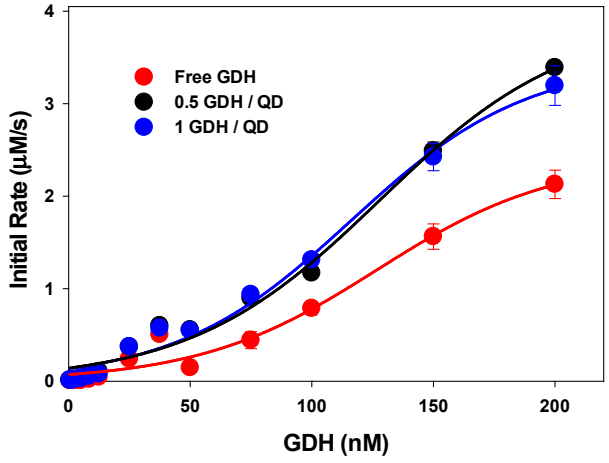


**Supplementary Figure S5.** Representative plot showing GDH activity as defined by the enzymes initial rate over a range of concentrations when either free in solution or as assembled with ratios of 0.5 and 1 GDH per QD. GDH initial rate showed an average increase of 136% for the 0.5 ratio while that of 1 ratio showed a 111% increase.

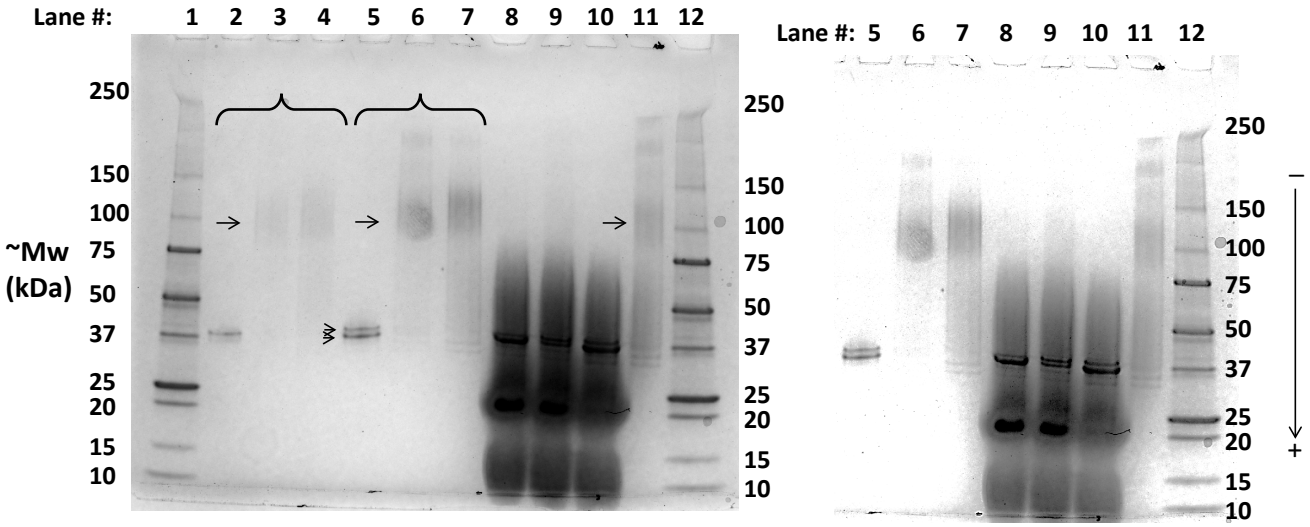


**Gel Contents: (Gel on right lanes 5-12 with different contrast setting to visualize dark bands)**
Lane 1 and Lane 12: Protein marker
Lane 2: GDH 5 pmol (bottom band/light) LDH 5 pmol (top band/dark)
Lane 3: GDH 5 pmol (bottom band/light) LDH 5 pmol (top band/dark) + QD 10 pmol
Lane 4: GDH 5 pmol (bottom band/light) LDH 5 pmol (top band/dark) + QD 40 pmol
Lane 5: GDH 20 pmol (bottom band) LDH 5 pmol (top band)
Lane 6: GDH 20 pmol (bottom band) LDH 5 pmol (top band) + QD 10 pmol
Lane 7: GDH 20 pmol (bottom band) LDH 5 pmol (top band) + QD 40 pmol
Lane 8: GDH 20 pmol (bottom band) LDH 5 pmol (top band) + QD 40 pmol GDH blocked
Lane 9: GDH 20 pmol (bottom band) LDH 5 pmol (top band) + QD 40 pmol LDH blocked
Lane 10: GDH 20 pmol (bottom band) LDH 5 pmol (top band) + QD 40 pmol GDH+LDH blocked
Lane 11: GDH 20 pmol (bottom band) LDH 5 pmol (top band) + QD 40 pmol separate assembly

**Supplementary Figure S6.** 4-12% gradient PAGE gel showing separation of GDH/LDH as free in solution at different concentrations and then as complexed to the indicated increasing ratio of QD. GDH migrates as the ~28 kDa monomer while LDH migrates as the 38.7 kDa monomer, rather than in their tetrameric forms. The QDs do not appear under the commassie blue staining used here. Upon addition of QD, a high molecule weight (MW) band of ~250 kDa appears for lanes 6,7 at the interface between the upper loading gel and bottom separation gel indicating protein aggregates that did not cross into the separating portion of the gel. Another smear of high MW species appear in lanes 3,4,6,7 between 75 and 150 kDa, which also gets darker with increasing QD presence. The protein monomer species also mostly disappear. These high MW species represent the different distributions of QD-LDH nanoaggregates or clusters. Lanes 8,9 selectively add blocking peptide to a preassembled protein-QD assembly in 200 fold excess and then add the other protein. In lane 8, more of the GDH is seen when it is blocked off the QD assembly, while in lane 9 it is the LDH that is seen when it is blocked. For lane 10, both GDH and LDH are seen as the QD is blocked there before the proteins are added. In lane 11, both proteins are added to separate but equal aliquots of QD and then the QD mixed before being run in the gel. It is also probable that enzymes that are somewhat 'loosely' associated with the clusters may get partially stripped from the nanocluster as they separate in the gel.

**Estimating Labeled Enzyme Incorporation into Clusters with FRET.** In a similar manner as we have previously described [4], we utilized Cy3 dyes (Cy3 monofunctional reactive dye, GE Healthcare) to labeled the different enzymes within the two enzyme cascade to experimentally approximate the number of labeled enzymes bound to the QD surface. The assays did confirm co-assembly while also again confirming that the average enzyme presence in each cluster differs from the assembly stoichiometry. It should be noted that the co-presence of multiple QD donors and dye-labeled acceptors in a nanoclustered structure complicate the interpretation of these results. For more in-depth description of the advantages and limitations of this technique, please see [4]. Briefly, a single enzyme was mixed with excess Cy3 dye overnight and then a Ni-NTA affinity column was run to remove the excess dye by washing the column repeatedly with 1X PBS and eluting the labeled enzyme with 1X PBS and excess imidazole. The labeled enzyme was then purified by dialysis against 50 mM phosphate buffer (pH 7.0) overnight to remove excess imidazole and any unlabeled dye, if present. Then UV-Vis spectra were taken of the labeled enzymes and the concentration of Cy3 dye was calculated from the absorbance at 552 nm. Using the 552 nm absorbance of the Cy3 dye, the predicted 280 absorbance for Cy3 was calculated and subtracted from the observed absorbance of the labeled dye at 280 nm. This difference in absorbance was then used to calculate the concentration of enzyme present using each enzyme's known molar extinction coefficient. Knowing the concentration of the enzyme within the labeled enzyme solution, various samples were made at increasing concentrations of enzyme where each were mixed with a constant concentration of QD (20 nM) and allowed to assemble for 2 hours. Then, these samples were used to create a FRET calibration curve where the increased FRET (quantified via QD emission) within the QD-labeled enzyme assembly correlated with increasing enzyme concentration. These curves assume the centrosymmetric distribution of the Cy3 around the QD remains valid through the enzyme range and in the presence of any QD clusters that may have formed. Next, batch mixtures of the two enzyme cascade system were prepared and assembled onto 520 QDs at comparable concentrations and ratios to those utilized throughout this study (1 LDH : 4 GDH) where only one enzyme in the mixture was labeled. This was done systematically for each enzyme in each of the cascades and the concentration of QD was kept constant at 20 nM. Using the FRET calibration curve for the labeled enzyme, the number of each labeled enzyme on the QD could be estimated. Representative data is shown below in **Supplementary Figures S7** and **S8.**

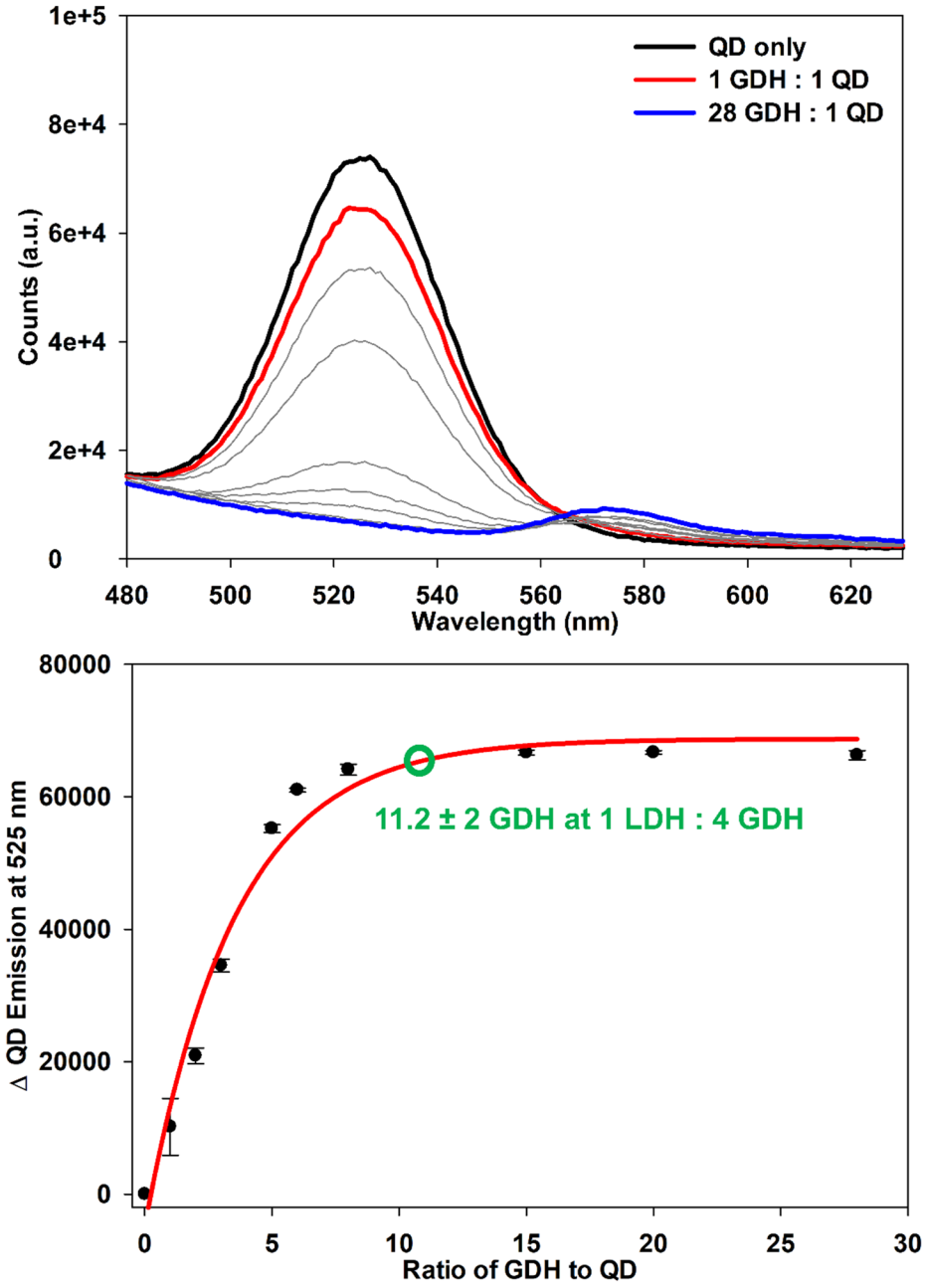


**Supplementary Figure S7.** Spectral characterization to determine number of bound enzymes in QD clusters. Samples were run in triplicate. (Top) Raw data of emission spectra for FRET calibration curve of 523 QD with increasing number of Cy3-labeled GDH enzymes. (Bottom) FRET calibration curve of 523 QD with increasing number of Cy3-labeled GDH enzymes. Data were fit to a nonlinear regression that was used to estimate the number of GDH enzymes in the two enzyme cascade mixture (green circle). Conditions for calibration curve include variable labeled GDH with 20 nM QD in 1X PBS (pH 7). Conditions for the two enzyme mixture (green) include 20 nM QD, 2.5 nM of non-labeled LDH, and 10 nM of the Cy3-labeled GDH.

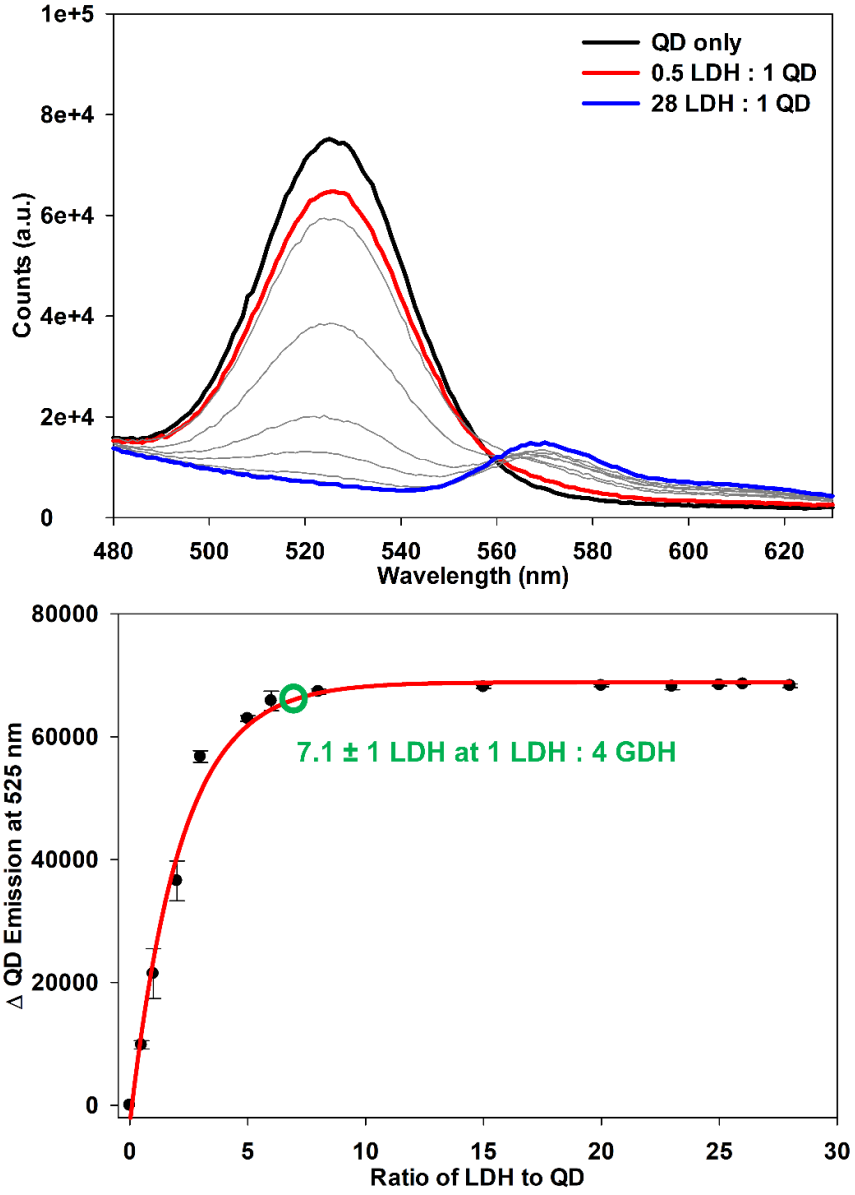


**Supplementary Figure S8** Spectral characterization to determine number of bound enzymes in QD clusters. Samples were run in triplicate. (Top) Raw data of emission spectra for FRET calibration curve of 523 QD with increasing number of Cy3-labeled LDH enzymes. (Bottom) FRET calibration curve of 523 QD with increasing number of Cy3-labeled LDH enzymes. Data were fit to a nonlinear regression that was used to estimate the number of LDH enzymes in the two enzyme cascade mixture (green circle). Conditions for the calibration curve include variable labeled LDH with 20 nM QD in 1× PBS (pH 7). Conditions for the two enzyme mixture (green) include 20 nM QD, 2.5 nM of Cy3-labeled LDH, and 10 nM of the non-labeled GDH.

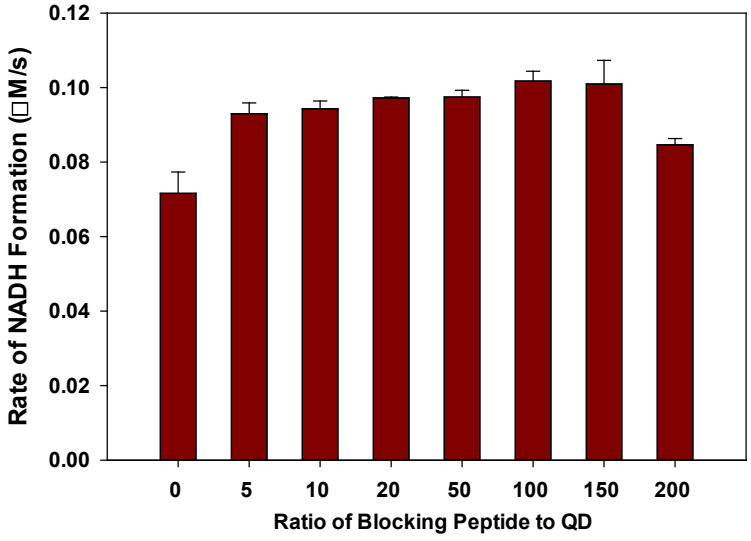


**Supplementary Figure S9.** Plot showing QD-GDH cluster activity as a function of increasing ratio of blocking peptide per QD.

**Compound Pricing**

As of early 2023, and according to Sigma Aldrich (Sigma Aldrich, St. Louis, MO, USA, https://www.sigmaaldrich.com/US/en), the following are relevant prices:

- NADH, that is β-nicotinamide adenine dinucleotide, reduced sodium salt hydrate, ≥ 97.0% HPLC, was $717.00/5g = $143.40/g = $101,727.96/mol using a molecular weight of 709.40 g/mol on an anhydrous basis.
- NADPH, that is β-Nicotinamide adenine dinucleotide 2′-phosphate reduced tetrasodium salt hydrate, =97% (dry weight), was $1650.00/g = $1,375,027.50/mol using a molecular weight of 833.35 g/mol on an anhydrous basis.
- D-(+)-Glucose, ≥ 99.5% GC, was $319/25kg = $0.01276/g = $2.2988416/mol using a molecular weight of 180.16 g/mol.
- The ratio between NADH and glucose on a per mol basis is therefore ~44,252.
- The ratio between NADPH and glucose on a per mol basis is therefore ~598,139.

We acknowledge prices fluctuate and will be different for different vendors and purities; we provide these here as a representative example.

**Supplementary References.**

1. J. C. Claussen, A. Malanoski, J. C. Breger, E. Oh, S. A. Walper, K. Susumu, R. Goswami, J. R. Deschamps and I. L. Medintz, *Journal of Physical Chemistry C*, 2015, **119**, 2208-2221.
2. Z. T. Johnson, N. Jared, J. K. Peterson, J. Z. Li, E. A. Smith, S. A. Walper, S. L. Hooe, J. C. Breger, I. L. Medintz, C. Gomes and J. C. Claussen, *Global Challenges*, 2022, **6**, 2200057.
3. J. N. Vranish, M. G. Ancona, E. Oh, K. Susumu, G. Lasarte Aragonés, J. C. Breger, S. A. Walper and I. L. Medintz, *ACS Nano*, 2018, **12**, 7911-7926.
4. J. C. Breger, J. N. Vranish, E. Oh, M. H. Stewart, K. Susumu, G. Lasarte-Aragones, G. A. Ellis, S. A. Walper, S. A. Diaz, S. L. Hooe, W. P. Klein, M. Thakur, M. G. Ancona and I. L. Medintz, *Nature Communications*, 2023, **14**, 1757.